JOURNAL OF PROPULSION AND POWER
Vol. 18, No. 2, March–April 2002

Linear Deterministic Source Terms for Hot Streak Simulations

Paul D. Orkwis*
University of Cincinnati, Cincinnati, Ohio 45221-0070
and
Mark G. Turner† and John W. Barter‡
General Electric Aircraft Engines, Evendale, Ohio 45215

Steady state surface rothalpy over specific heat at constant pressure (temperature units) results obtained with a linear unsteady solution-based lumped deterministic source term are compared with results obtained from a traditional, nonlinear, inviscid unsteady solution for an aircraft engine first stage high-pressure turbine rotor configuration. The relationship between the source terms and traditional solution variables is explored to offer a unique insight into comparing the two approaches. Boundary condition/potential field effects and the order of accuracy of the available schemes are also explored and show a significant effect on surface rothalpy results. The new technique demonstrates a significant potential for approximately including unsteady hot streak effects in time average calculations with minimal computer effort.

Introduction

COMPUTATIONAL fluid dynamics (CFD) has progressed rapidly in the past two decades for turbomachinery applications. From stream surface techniques the state of the art has progressed to fully three-dimensional coupled-blade-row nonlinear viscous calculations for virtually all gas turbine components. These advances now permit blade-row designs in three dimensions and are rapidly advancing to the point where three-dimensional multistage unsteady analyses might be the norm sometime in the next decade.

Until that point, unsteady flow physics will be relegated to post-design analyses, and rule-of-thumb-based design practice will be required when considering unsteady effects. This is unfortunate because blade-row-to-blade-row interaction effects, such as clocking, will not be accounted for in design phase simulations. One particularly interesting unsteady effect not currently accounted for is rotor temperature segregation caused by combustor hot streaks and upstream cooling wakes.

Preferential surface heating and phantom cooling are names sometimes used to describe these unsteady phenomena. Another name associated with hot streak surface heating is the Kerrebrock–Mikolajczak[1] effect. These researchers were the first to describe why unsteady effects associated with compressors lead to increased pressure side heating. This effect is even more pronounced in turbines as a result of larger circumferential temperature variations. The description of the effect is based on the fact that the flow in combustor hot streaks has essentially the same Mach number as the surrounding fluid, but is, in general, much hotter because of the combusting gases. This means that the fluid itself must have a higher velocity than the surrounding flow. These circumferential variations in flow properties would provide no additional basis for heating if it were not for the fact that adjacent blade rows move relative to one another. The hot streak enters the blade row at a higher relative flow angle than the surrounding fluid when viewed in the rotating-blade reference frame. Kinematic arguments then suggest that the hot fluid should have a preference toward the pressure side of the rotor, thereby increasing the average temperature experienced by that side of the rotor above that predicted by mixing plane analyses.

Typical mixing plane or steady multistage analyses do not simulate the effect of this unsteady phenomenon because they smear the circumferential variations and thereby obliterate the basis for the effect. Unsteady calculations are the only apparent hope for including the effect of hot streaks in the solution. Unsteady CFD codes are currently capable of simulating the phenomena but are generally too slow in reaching cyclic convergence to be of use in an overnight design time frame. Progress is rapidly being made to improve the efficiency of these schemes, but their use in a day-to-day design sense is probably still a few years off.

What is needed at the present time is a way to include the effect of unsteadiness in a steady solver, if even in an approximate sense. Deterministic source terms (DST) offer a possible approach to solving this problem. In this idea a source term is inserted into the governing equations that mimics the effect of some unsteady phenomena. This is similar to the way turbulence (the ultimate unsteady phenomena) is modeled through the Reynolds-averaged Navier–Stokes (RANS) approach.

To explain the preceding analogy, start by considering the model of turbulence assumed in the RANS approach. The random fluctuations of turbulence are modeled via a point-wise turbulent viscosity coefficient μ_T that augments the physical diffusion term. Hence, turbulent diffusion is assumed to follow a similar functional form as physical diffusion. In the DST approach a point-wise source term is used to represent the time averaged effect of unsteadiness in the steady system; however, in this case no assumption is made a priori regarding the relationship between the unsteady phenomena and that occurring in the time averaged flowfield. The major difference between the two approaches is the form of the function used to model the phenomena (a fact expanded upon in a later section). However, the two techniques are similar in that unsteady effects not resolved by the simulation can be included through point-wise equation modifications.

The lumped deterministic stress (LDS) approach has been developed in the past few years[2,3] to determine the form of the unsteady source term from fully unsteady solutions. The idea can be applied in a postdictive sense once the more detailed solution is known. Modeling of these terms can be developed after large numbers of cases have been computed and a general understanding of the source terms is obtained.

A variation of this approach has been employed recently by Busby et al.,[3] who used a lower-fidelity (inviscid) set of equations to compute approximate source terms in a relatively short time. Their work

Received 26 July 2000; revision received 18 December 2000; accepted for publication 25 August 2001.

*Associate Professor, Department of Aerospace Engineering and Engineering Mechanics. Senior Member AIAA.
†Senior Staff Engineer, Aero and Aster Model Technology. Senior Member AIAA.
‡Lead Engineer, Engineering Tools Development. Senior Member AIAA.

showed that inviscid analyses faithfully approximate the hot streak unsteadiness source terms.

An even more aggressive approach would be to utilize linear unsteady techniques to determine the source terms. These techniques have been used extensively for aeromechanics problems and can produce reasonable unsteady flowfields in a fraction of the computer time as compared to nonlinear analyses. The difficulty with the approach is that the perturbations from the steady state solution are linear in nature, hence, they do not include the full unsteady flow physics.

Although linear, these techniques do offer a reasonable approximation to the unsteady perturbation flowfield. It is proposed in this paper that, rather than use them to directly compute the unsteady flowfield, they could be used to offer an even quicker way to approximate the DST than nonlinear unsteady inviscid analyses (see Ref. 4). This idea was also suggested by the works of Giles,[5] Fritsch,[6] and van de Wall.[7] The purpose of this paper is to compare how well the linear solvers work as compared to the nonlinear unsteady approaches. In light of the recent work reported by Busby et al.,[3] it is sufficient to demonstrate the technique through comparisons of results obtained with inviscid solutions.

The following sections demonstrate this concept by first describing the governing equations that permit the calculation of the DST. Next the nonlinear and linear solvers employed in this work are described. The paper then discusses the results obtained with the two approaches and ends with a final summary.

Deterministic Source Terms

Deterministic source terms offer a means to include the effects of solution unsteadiness in time mean computations. They can be derived exactly in a postdictive manner once an unsteady solution has been obtained. Predictive models of the source terms can be generated once the general behavior of the unsteady effects has been characterized and as such are not the focus of the current paper. The easiest way to understand how the DST can be obtained is to follow their general derivation, as described next.

Consider the general form of the unsteady energy equation (written in two dimensions) for inviscid, nonheat conducting flow:

$$\frac{\partial(\rho I)}{\partial t} + \frac{\partial(\rho I u)}{\partial x} + \frac{\partial(\rho I v)}{\partial y} + \frac{\partial p}{\partial t} = 0 \tag{1}$$

where I is the rothalpy, p is the pressure, and u and v are velocity components. Rothalpy was chosen as the energy equation variable for this work because it is the conserved quantity for the rotor relative reference frame. It is not the only variable to consider when studying hot streak flow physics, but offers the advantage of avoiding nonconserved variable numerical errors.

Nonlinear unsteady solution techniques obtain the time history of energy from Eq. (1) by moving the spatial derivatives to the right-hand side (RHS) and discretizing, that is,

$$\frac{\partial(\rho I)}{\partial t} = -\left[\frac{\partial(\rho I u)}{\partial x} + \frac{\partial(\rho I v)}{\partial y} + \frac{\partial p}{\partial t}\right] \tag{2}$$

The same equations are used to solve for steady state solutions, in which Eq. (2) is used to relax the solution to a steady state, that is, left-hand side (LHS) = 0. An equivalent way to describe this approach is to call the RHS of Eq. (2) the negative of some residual $R(Q)$ and drive that residual to zero. This last description will take on greater meaning later.

Equation (2) is the governing equation for unsteady inviscid flows. It continues to govern the unsteady fluid mechanics even if the variables are decomposed into separate components. The typical DST decomposition begins by splitting variables into their deterministic and stochastic components, that is, $q = \bar{q} + q'$. Where $\bar{q}$ is the deterministic portion and q' is the stochastic. The latter component is then modeled using some sort of turbulence model, whereas the former can be simulated by the technique. If the stochastic components are ignored (because they are represented by turbulence models and the test case is assumed inviscid), the next step in the derivation is to split the deterministic quantity $\bar{q}$ into a mean value $\bar{\bar{q}}$ and a deterministic fluctuation q''. If these expressions are substituted into Eq. (2) and the stochastic fluctuations are ignored, the equation can be rewritten as

$$\frac{\partial(\overline{\overline{\rho I}} + \rho I'')}{\partial t} = -\frac{\partial\lfloor(\overline{\overline{\rho I}} + \rho I'')(\bar{\bar{u}} + u'')\rfloor}{\partial x} - \frac{\partial\lfloor(\overline{\overline{\rho I}} + \rho I'')(\bar{\bar{v}} + v)\rfloor}{\partial y} - \frac{\partial(\bar{\bar{p}} + p'')}{\partial t} \tag{3}$$

Equation (3) is simply a restatement of Eq. (2). It can be further expanded into

$$\frac{\partial(\overline{\overline{\rho I}} + \rho I'')}{\partial t} = -\left[\frac{\partial(\overline{\overline{\rho I}}\,\bar{\bar{u}})}{\partial x} + \frac{\partial(\overline{\overline{\rho I}}\,v)}{\partial y} + \frac{\partial\bar{\bar{p}}}{\partial t}\right] - \left[\frac{\partial(\overline{\overline{\rho I}}\,u'')}{\partial x} + \frac{\partial(\overline{\overline{\rho I}}\,v'')}{\partial y} + \frac{\partial p''}{\partial t}\right] - \left[\frac{\partial(\rho I''\bar{\bar{u}})}{\partial x} + \frac{\partial(\rho I''\bar{\bar{v}})}{\partial y}\right] - \left[\frac{\partial(\rho I''u'')}{\partial x} + \frac{\partial(\rho I''v'')}{\partial y}\right] \tag{4}$$

The time average of the LHS and the second and third brackets on the RHS are identically zero by definition once Eq. (4) is time averaged. Hence, the governing equation (to be solved) for the time average of a flow with unsteady perturbations is

$$0 = \overline{\overline{-\left\{\frac{\partial(\overline{\overline{\rho I}}\,\bar{\bar{u}})}{\partial x} + \frac{\partial(\overline{\overline{\rho I}}\,\bar{\bar{v}})}{\partial y}\right\}}} - \overline{\overline{\left\{\frac{\partial(\rho I''u'')}{\partial x} + \frac{\partial(\rho I''v'')}{\partial y}\right\}}} \tag{5}$$

or

$$0 = \overline{\overline{-R(\bar{\bar{Q}})}} + \mathrm{DST} = -R(\overline{\overline{Q}}) + \mathrm{DST} \tag{6}$$

Bracket one in Eq. (5) is the same residual solved for the steady state by relaxation methods [(for example, see Eq. (2)]. This term is already a mean quantity; hence, the time average is redundant. Bracket two represents the source terms that must be added to the steady equations to include the effect of unsteadiness.

It should be recognized immediately that the solutions obtained from Eqs. (2) and (5) will be different and will, respectively, give the steady state and time averaged solutions, provided the correct DST is applied in the latter. The problem then becomes determining the correct form of the DST.

DST from Nonlinear Solutions

If one considers a typical nonlinear unsteady solver for turbomachinery flows, like the MSU TURBO code,[8,9] the approach to obtaining the DST becomes apparent by considering Eq. (5). This is because nonlinear unsteady codes solve Eq. (2) directly; hence, upon time averaging the solution, Eq. (5) is solved by definition. Therefore, one simply needs to time average the unsteady solution and substitute it into the steady state residual function $R(Q)$ to determine the DST. This approach is sometimes known as LDS because all of the individual components of the DST are "lumped" together. This approach is particularly convenient because it involves only the calculation of a single residual function. This essentially is the approach taken by Busby et al.[3] and was the route chosen in the current work for finding the LDS obtained from the nonlinear unsteady TURBO code.

DST from Linear Solutions

At first glance it might appear that solutions from linear approaches could not possibly be used to determine the LDS because it is the nonlinear interaction between unsteady perturbations that

leads to effects like temperature segregation. That is, unsteady temperature fluctuations are carried by unsteady velocity perturbations for flows with hot streaks. Whereas in linear unsteady approaches the perturbations are carried by the base flow, not by the coupled perturbed variable field.

To better understand this, consider first how the specific form assumed for the unsteadiness leads to the governing equations for linear unsteady solvers. These techniques solve for each perturbation frequency separately by imposing a Fourier series representation of the temporal solution and linearizing the resulting equations. Complex numbers in the exponential form represent the series. The Fourier-series transforms the equations from a set of unsteady nonlinear real variable equations to a set of steady state linear complex variable equations. Therein lies the advantage of these schemes: the unsteady solution for each discrete frequency is obtained in a multiple of the time required to obtain steady state results (typically about twice as long), and the linear perturbation assumption allows each frequency to be solved in parallel. This results in a considerable time reduction as compared to that needed for a nonlinear unsteady approach.

Unfortunately the solutions obtained in this manner do not satisfy Eq. (5) exactly, but satisfy an approximate set of complex perturbation equations (which will not be repeated here for brevity[10]). Perturbation products are themselves defined to be zero under the small perturbation assumption. Therefore, Eq. (5) is not itself satisfied by a linear unsteady approach. This causes a significant setback for the LDS approach because the first bracket in Eq. (5) is already effectively zero (as it represents the base flow) and cannot be used to form the deterministic source terms.

However, the DST can be reconstructed from the linear perturbation solution even though the linear solution procedure assumes away the perturbations. This is possible if the perturbations are a reasonable approximation of the actual nonlinear solution. In that case, even though the perturbations are themselves linear, a superposition solution can be created from the nonlinear base flow plus linear perturbation variables and Eq. (5) can be satisfied approximately. The DST in Eq. (5) is clearly nonlinear even if it is approximated by originally linear perturbations.

Therefore, the approach required for determining the LDS from a linear solver uses the time average of the nonlinear steady state residuals obtained with the base flow plus linear perturbation solutions. It is in effect only the order in which the calculations are performed that changes.

Nonlinear Solutions

Step 1) Time average the unsteady solution variables.

Step 2) Compute the steady state residual.

Linear Solutions

Step 1) Compute the steady state residual from the instantaneous base flow plus perturbation solution.

Step 2) Time average the residuals.

The LDS obtained from nonlinear solutions are exact (within truncation error and assuming cyclic convergence), whereas the LDS obtained from linear solutions will only be approximate. The accuracy of the latter depends upon the validity of the linear perturbation solutions. However, as will be demonstrated in the results, the individual perturbation components are reasonably accurate and provide a good approximation of the LDS.

The key issue to understand when viewing the LDS contours is the meaning of their spatial distribution. Strictly speaking, the values of these terms represent redistributions of conserved quantities, not additional mass, momentum, or rothalpy (energy). These changes are then convected along the streamlines to the rest of the solution. So that given a flow with locally higher temperature that returned downstream to a lower temperature, the LDS field would reflect this by being positive as the temperature increased and then negative as it decreased. It is then the integrated effect, in a substantial derivative sense, that becomes important.

Unsteady Solution Techniques

The solutions obtained from two distinct unsteady techniques are compared in this work. The first unsteady solution technique is a typical nonlinear unsteady code and the second a linear unsteady code of the type usually employed in aeromechanics analyses. The latter technique is more computationally efficient, but suffers from being approximate in nature.

Nonlinear Approach

The nonlinear code employed in this work is the MSU TURBO algorithm of Chen et al.[8] and Chen and Barter.[9] The technique can be run as a fully coupled stage solver or as an individual blade-row solver with unsteady boundary conditions. The technique is a Gauss–Seidel-based approximately factored implicit scheme that solves the spatial fluxes with Roe's flux difference splitting. This offers several choices of spatial discretizations, including second- and third-order upwind schemes and a central difference option. Newton subiterations are used at each time step to minimize linearization errors caused by discretization. One-dimensional characteristic boundary conditions are employed. Single-processor run times on a Cray J90 for calculations similar to those required in the current work are on the order of several days before the solution integrated in time will reach a cyclic state.

Linear Approach

The linear code employed in this work is the GE TACOMA code of Holmes, and Mitchell.[10] It solves for linear perturbations to a nonlinear base flow. Both the linear and nonlinear portions of the code employ a second-order Jameson-type central differencing scheme.

This code gains its efficiency from an assumption about the form of the unsteadiness. In this case the temporal unsteadiness is represented by a Fourier-series description, which can be written in the exponential form of the complex valued function. When this is done, the time derivative is removed from the system. Then, instead of solving for an unsteady time history of a real valued function, one solves for the steady state of a complex valued function. In addition, perturbation products are ignored so that the perturbations themselves become functions of a linear operator.

The nonlinear steady code changes very little to form the linear perturbation code because the very same implicit operators are employed as for a steady state nonlinear solution. A Runge–Kutta integration technique with central differences and residual averaging is used, and characteristic based boundary conditions are employed.

The solver becomes many times faster (approximately 20-25 on the same machine) than the corresponding unsteady nonlinear solution because of the change in variables and perturbation product assumptions. Typical run times on a C160 processor based HP workstation are only a few hours for the single harmonic problems tested in this work, effectively twice as long as a steady state solution on the same grid. Multiple harmonics can be computed independently and superposed because the problem is linear. (Currently the linear unsteady code does not define and parse out the multiple harmonic problems to other machines; the process is handled by scripting tools. However, this can be included easily in future when the approach matures. The important point is that many harmonics can be computed at the same time on different processors/machines and their results brought together thereafter). Hence, apart from the small overhead increase from the superposition of solutions, the process is inherently parallel and does not represent a serial bottleneck. In addition, both the linear and nonlinear codes can be made parallel in a similar manner, hence, that aspect of speed up is common and of no consequence to the comparison. In total, the effective work required for the linear DST approach is about one fifth that of a comparable nonlinear scheme. A consequence of this is that the new approach easily satisfies an overnight turnaround requirement in a workstation environment and is efficient enough for design-type applications.

The unsteadiness is passed between blade rows by transforming the spatial nonuniformities in the circumferential direction into their corresponding temporal variations in the rotating reference frame.

A Fourier-series is then performed to determine the appropriate discrete frequencies that exist in the solution. A linear solution is solved for each existing frequency and the full unsteady solution developed by superposition once the solution associated with each frequency is obtained.

The solutions obtained with both approaches are presented next.

Results

The goal of this research was to demonstrate the efficacy of an LDS source-term-augmented steady state solution procedure. Previous researchers[2] have shown that the LDS approach works when derived from the exact nonlinear unsteady viscous equations and also when inviscid nonlinear unsteady solutions are used in fully viscous problems.[3] Hence, it is sufficient to compare the time averaged nonlinear unsteady inviscid solution to the source term augmented steady state inviscid solution. That comparison is presented in this section.

The particular test case was a typical modern first-stage high-pressure turbine geometry. Equal numbers of rotors and stators were assumed; hence, the flow was periodic spatially in the circumferential direction. This was done so that the nonlinear solution could be obtained in a reasonable amount of time.

The combustor hot streak was modeled crudely as a blade-passing frequency sinusoidal disturbance in velocity and density (but not pressure). The maximum magnitude of the perturbations was 10% in density and 5% in velocity as compared to the circumferential average values. The radial profile of perturbation amplitude is shown in Fig. 1. The two disturbances are 180 deg out of phase so as to replicate crudely a combustor hot streak consisting of a region of increased temperature and velocity.

Two H-grids were employed for the test cases: a grid typical of standard design analyses consisting of $32 \times 32 \times 128$ cells and a grid with greater upstream extent that employed $32 \times 32 \times 144$ cells. One-dimensional characteristic based boundary conditions were employed, but the implementation was different in the linear and nonlinear unsteady approaches.

Also different between the two approaches were the spatial discretizations. The linear approach employed only a Jameson-type central differencing, whereas the nonlinear scheme employed Roe-type flux difference splitting. Several different spatial schemes can be developed from the upwind approach, and three were employed in the current work: a third-order accurate scheme, a second-order upwind scheme, and a central-difference-typescheme.

The results are divided into three separate topics. First, a general description of the LDS terms is presented to demonstrate their similarity. Second, results are presented to show how upstream influence coupled with boundary condition differences affect solution behavior. Finally, differences associated with spatial discretization are explored. The general figure of merit in all discussions is the value of the normalized surface rothalpy, the conserved energy quantity in a rotating reference frame (see Ref. 11). In all cases the rothalpy was normalized by its freestream value.

LDS Terms

The comparison between the lumped deterministic source term results obtained with the linear and nonlinear techniques is the launch point for demonstrating the efficacy of the proposed approach. A reasonable comparison between these quantities is indeed a necessary condition for the approach to be successful. An earlier work by the authors[4] demonstrated that the two approaches develop similar LDS profiles. Figures 2a and 2b present the respective energy LDS results for the linear and nonlinear techniques. In-depth discussion of the results is left to the reference, however, it is important to note that the major required features of the LDS are very nearly identical in the two cases.

In particular, the band of high DST beginning upstream of and connecting to the stagnation region and then extending downstream through the passage is quite evident. This DST is the primary reason for increased surface rothalpy (temperature) inherent in unsteady hot streak flow physics. Both solutions demonstrate, as one travels through the passage from suction to pressure side, a "cool" DST region near the suction side, the above "hot" DST, a peninsula of near-zero DST, and lastly a small streak of high DST near the pressure surface. This three-dimensional DST field must be coupled with the time averaged streamlines to define how the axisymmetric inflow rothalpy is modified by unsteadiness to produce surface hot spots.

The next important point to be considered is how potential effects interact with the boundary conditions to affect both the solution and the "imposed" solution variables.

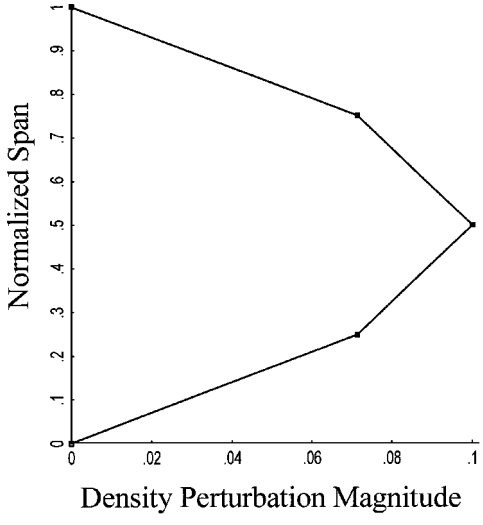

Fig. 1 Radial distribution of inflow density perturbation magnitude in units of percent circumferential average density.

Fig. 2a Lumped deterministic energy at midspan obtained from third-order TURBO code.[4]

Fig. 2b Lumped deterministic energy at midspan obtained from the linear unsteady TACOMA code.[4]

Boundary Condition Effects

The interaction between upstream potential influences and boundary condition specification is critically important to the success of a hot streak simulation because small angle changes can greatly affect the kinematics of the flow. This is not a new effect and has been observed in steady state solutions for some time. However, in the current approach both the linear and nonlinear techniques are applied as single blade-row solvers with an imposed perturbation reminiscent of what one might expect from a real engine hot streak. The first grid satisfies the conventional steady-state wisdom as to proper upstream extent to avoid potential field effects, while the second employed a small grid extension upstream of the leading edge. As will be demonstrated in the next series of figures, this can have quite an impact on the resulting surface rothalpy values and can give insight into potential field effects.

Recall that the imposed perturbation was 10% in density and 5% in velocity. However, upstream potential effects can alter the specification of the perturbation boundary condition when the one-dimensional Riemann conditions are satisfied. As shown in Fig. 3a, the absolute flow angle variations are reduced for both techniques with the upstream grid extension. These effects can be directly attributed to the upstream potential field as demonstrated by the static-pressure results shown in Fig. 3b. Combined the two plots indicate that the grid extension is required to minimize differences between the schemes. Recall that potential influences decay exponentially; hence, the inflow perturbation amplitude reductions demonstrated by both solvers are sufficient to ensure that the extended grid is sufficiently far upstream so as to minimize these effects. The linear technique is apparently more greatly affected by the potential field. However, the surface rothalpy results for both cases are significantly affected, as illustrated in the surface rothalpy contours presented next. The current results then bring into question the extrapolation of steady state knowledge for unsteady solutions and point to perhaps a greater impact of transient upstream potential effects than might otherwise be expected in a typical steady state analysis.

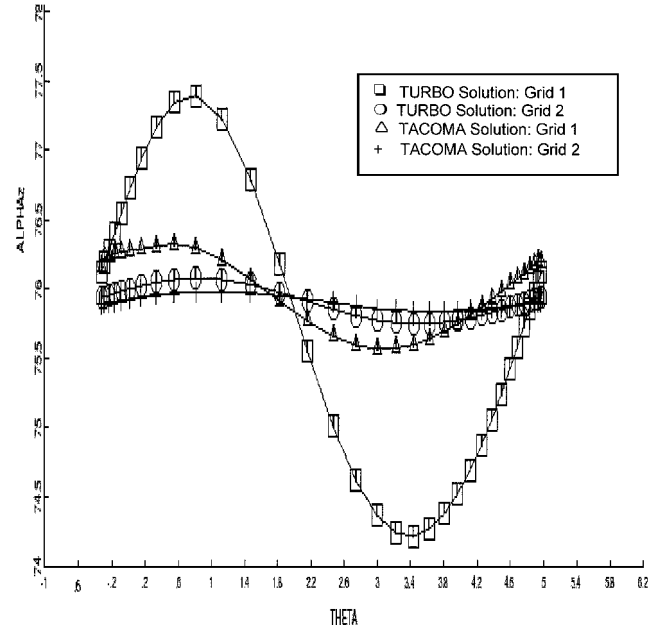

Fig. 3a Absolute flow angle variation in the tangential direction for the time-averaged third-order TURBO and LDS steady state TACOMA analyses with both the standard and extended grids.

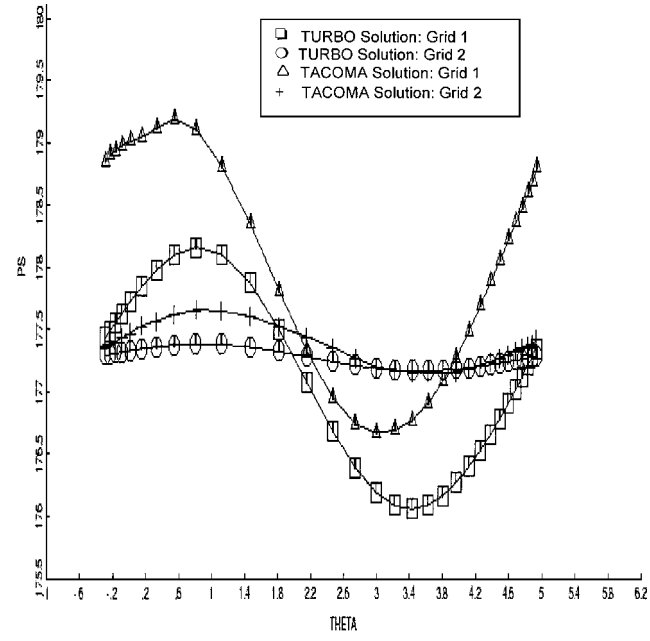

Fig. 3b Static-pressure variation in the tangential direction for the time-averaged third-order TURBO and LDS steady state TACOMA analyses with both the standard and extended grids.

Figures 4–7 illustrate the pressure-side-surface rothalpy differences for the four respective test cases just discussed. Both techniques produce dual local rothalpy maxima and tip-wise radial migration. It is apparent that the rothalpy maximum results for both techniques are reduced significantly with the grid extension. A very considerable change occurs in the time averaged TURBO results, and a smaller, but not insignificant change, occurs in the TACOMA solutions. Unfortunately, the values are under predicted by at least 37% with the linear technique, and the extent of the downstream and radial migration is also underpredicted. However, the extended

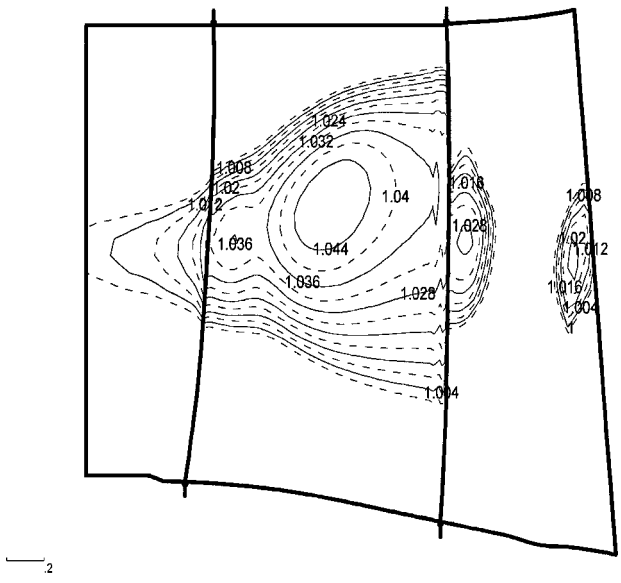

Fig. 4 Time averaged pressure side normalized surface rothalpy obtained with the third-order TURBO code on the standard grid.

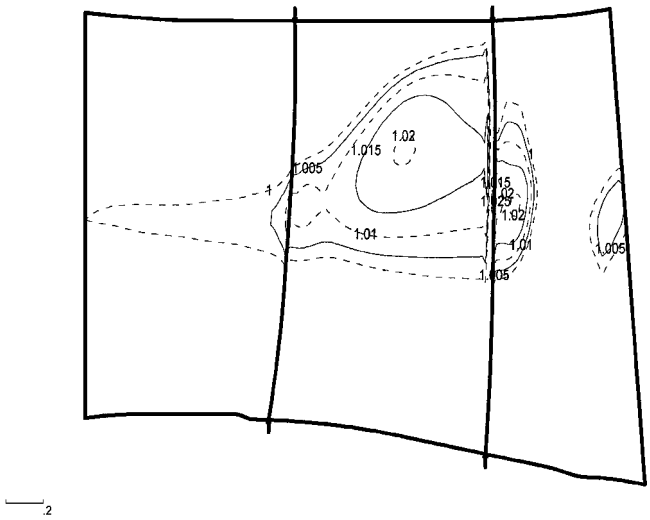

Fig. 5 Time averaged pressure side normalized surface rothalpy obtained with the third-order TURBO code on the extended grid.

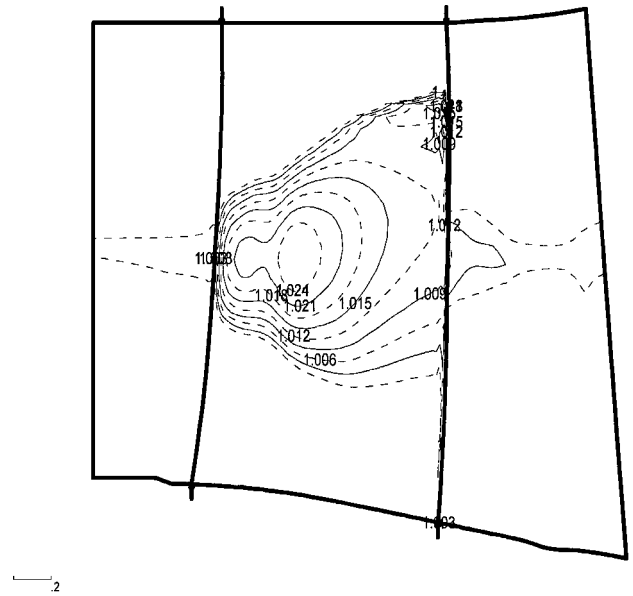

Fig. 6 Time averaged pressure side normalized surface rothalpy obtained with the LDS steady state TACOMA code on the standard grid.

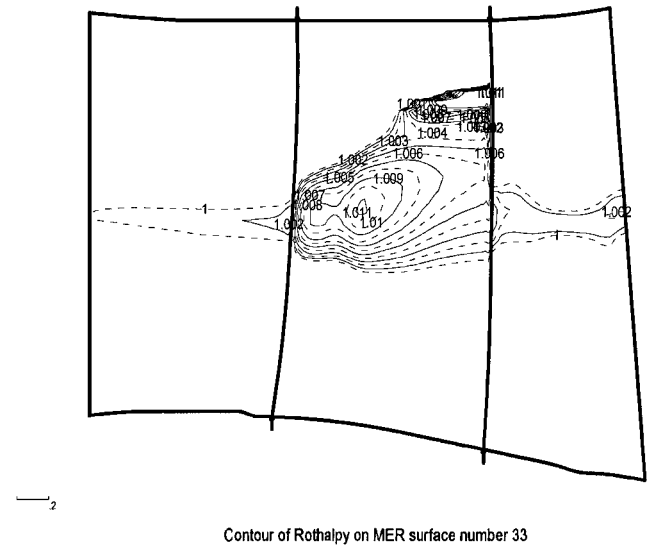

Fig. 7 Time averaged pressure side normalized surface rothalpy obtained with the LDS steady state TACOMA code on the extended grid.

grid results obtained with the two techniques are much closer than that obtained with the original grid. An explanation of these results appears to be the relatively dissipative central difference technique used in the TACOMA solver as compared to the third-order differencing used in TURBO. This assertion will be demonstrated in the next section.

Spatial Discretization Effects

It was not apparent in the LDS terms presented earlier, but the order of discretization accuracy appears to have a significant effect on the analysis of hot streak flow physics. The algorithm employed for the linear solver is essentially fixed as a second-order central-difference technique. However, the nonlinear TURBO scheme employs a Roe flux difference solver, and, as such, offers several discretization accuracies from which to choose. Typical unsteady nonlinear solutions are obtained with a third-order accurate upwind scheme, whereas lower order variants are typically not reported. This might be because of the striking solution changes that this accuracy drop entails.

Figures 8 and 9 show the surface rothalpy results obtained with the second-order upwind and central-difference schemes available in TURBO and obtained on the upstream-extended grid. These results should be compared with Figs. 5 and 7 for the third-order TURBO and TACOMA results, respectively. The results obtained with the reduced accuracy discretizations demonstrate that the linear technique is quite adept at computing the value of maximum surface rothalpy, when like order of accuracies are compared. The least accurate TURBO scheme (second order upwind) provides a peak rothalpy value that is identical to that obtained with the linear source term solver.

Unfortunately, the radial migration of the hot streak is not computed as well as one might hope with the linear source term technique. This issue is still being studied and might again be related to the discretization, as the use of primitive variable pressure might adversely affect the LDS momentum source term generation during the time averaging process.

In spite of the radial migration discrepancies, the linear perturbation-based LDS source terms appear to offer a reasonably accurate approximate surface rothalpy calculation technique that can

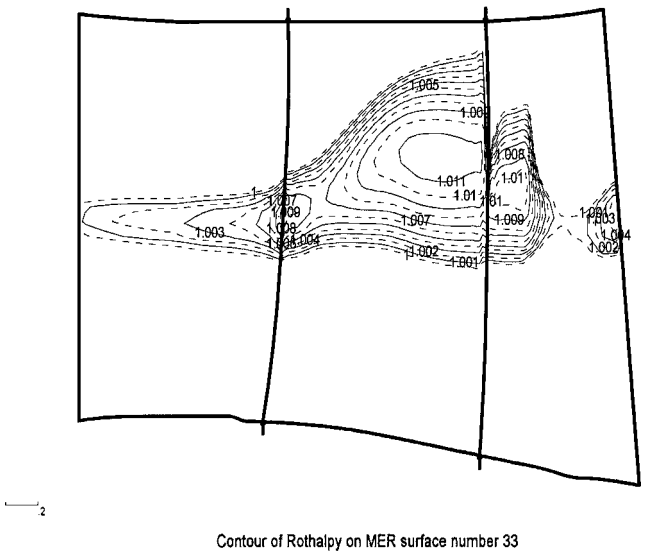

Fig. 8 Time averaged pressure side normalized surface rothalpy obtained with the second-order upwind TURBO code.

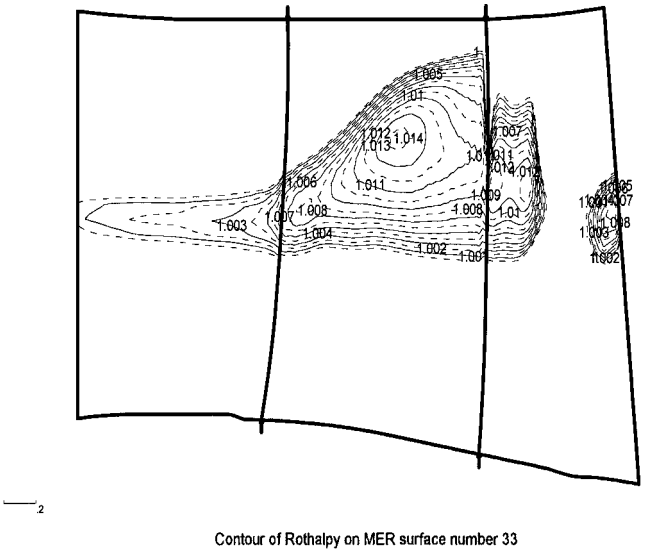

Fig. 9 Time averaged surface rothalpy/*Cp* obtained with the central difference TURBO code.

obtain solutions quickly enough to be applicable to the designer. The advantage of this technique is the timely way that an estimate of the unsteady temperature segregation flow physics effects are obtained, as compared to a brute-force unsteady nonlinear analyses. Results can also be obtained with viscous perturbations, an exercise that will be left for future studies.

Conclusions

A new linear unsteady perturbation-based source term technique for steady state hot streak simulations was presented and compared to a traditional, unsteady nonlinear solver. The source terms representing the preferential heating on the pressure side of the rotor were well represented by the linear approach. Upstream potential influences coupled with boundary condition implementations were found to affect considerably the surface rothalpy results in both techniques. Spatial discretization accuracy was also found to affect significantly the surface rothalpy results. However, the linear technique solutions compared quite favorably with the traditional approach when these effects were minimized. Maximum surface rothalpy values were predicted well, although the radial migration of the hot streak was underpredicted. In spite of that, the potential time-savings for unsteady analyses were made apparent by these results and indicate that the technique can be a valuable tool for including the effects of hot streak unsteadiness in design analyses.

Acknowledgments

This work was partially supported under the NASA AST Program, Contract NAS3-27720, AOI 5, monitored by Bob Boyle and John Rhodi, and by sabbatical leave support from the University of Cincinnati. The authors would also like to thank John Adamczyk for his knowledgeable input into hot streak modeling. Finally, the first author would like to thank the entire Analytical Aerodynamics and Cooling Technology/Engineering Tools Development Subsection team at General Electric Aircraft Engines and Managers Richard Cedar and Christopher B. Lorence for their help, support, and encouragement during his sabbatical year residence.

References

[1] Kerrebrock, J. L., and Mikolajczak, A. A., "Intra-Stator Transport of Rotor Wakes and Its Effect on Compressor Performance," *Journal of Engineering for Power*, Vol. 92, No. 4, 1970, pp. 359–368.

[2] Sondak, D. L., Dorney, D. J., and Davis, R. L., "Modeling Turbomachinery Unsteadiness with Lumped Deterministic Stresses," AIAA Paper 96-2570, July 1996.

[3] Busby, J., Sondak, D., Staubach, B., and Davis, R. L., "Deterministic Stress Modeling of Hot Gas Segregation in a Turbine," American Society of Mechanical Engineers, Paper 99-GT, June 1999.

[4] Orkwis, P. D., Turner, M. G., and Barter, J. W., "Deterministic Stress Source Terms for Turbine Hot Streak Applications Derived from Linear Unsteady Solutions," International Symposium on Air Breathing Engines, Paper IS-7143, Sept. 1999.

[5] Giles, M., "An Approach for Multi-Stage Calculations Incorporating Unsteadiness," American Society of Mechanical Engineers, Paper 92-GT-282, June 1992.

[6] Fritsch, G., "An Analytical and Numerical Study of the Second-Order Effects of Unsteadiness on the Performance of Turbomachines," Ph.D. Dissertation, Massachusetts Inst. of Technology, Dept. of Aeronautics and Astronautics, Cambridge, MA, April 1992.

[7] Van de Wall, A. G., "A Transport Model for the Deterministic Stresses Associated with Turbomachinery Blade Row Interactions," Ph.D. Dissertation, Dept. of Mechanical and Aerospace Engineering, Case Western Reserve Univ., Cleveland, Jan. 1999.

[8] Chen, J. P., Celestina, M. L., and Adamczyk, J. J., "A New Procedure for Simulating Unsteady Flows Through Turbomachinery Blade Passages," American Society of Mechanical Engineers, 94-GT-151, June 1994.

[9] Chen, J. P., and Barter, J., "Comparison of Time-Accurate Calculations for the Unsteady Interaction in Turbomachinery Stage," AIAA Paper 98-3292, July 1998.

[10] Holmes, D. G., and Mitchell, B. E., "Navier–Stokes Calculations for Flutter and Forced Response," *Unsteady Aerodynamics and Aeroelasticity of Turbomachines*, edited by T. H. Fransson, Kluwer Academic, Norwell, MA, 1998, pp. 211–224.

[11] Lyman, F. A., "On the Conservation of Rothalpy in Turbomachines," American Society of Mechanical Engineers, 92-GT-217, June 1992.